Fast And Accurate Soft-Switching And Hard-Switching Losses Estimation For Power Converter, Application To The Dual Active Bridge (DAB) Converter

Francois Boige, Nicolas Videau, Adel Ziani, Bruno Guerrero, Julien Laclaverie
Gamma Technologies
601 Oakmont Ln, Westmont, IL 60559, US
f.boige@gtisoft.com
www.gtisoft.com

Keywords

«Converter Design», «Resonant Converter», «Soft Switching», «Zero-voltage Switching», «Dual Active Bridge (DAB)»

Abstract

This paper presents an integrated method and workflow to estimate Dual Active Bridge (DAB) DC/DC converter semiconductor loss in losses both in soft-switching including Zero-Voltage Switching (ZVS), Zero-Current Switching (ZCS) and hard-switching. The method uses soft-switching and hard-switching energy look-up table with a frequential solver to estimates DAB loss. In case, the switching energies are not available, a virtual double pulse simulation is performed based on the datasheet characteristic. The comparison with the literature display a very fast computation time with a reasonable trade-off in accuracy.

Introduction

Electric vehicle, large-scale storage of electrical energy in batteries, photovoltaic energy, aircraft onboard power grid, etc. require the use of galvanically insulated electrical energy converters to guarantee the safety of goods and people. To accompany the growth of these applications the converters must be as much as possible cost-effective with a high efficiency. Faced with these objectives and regulatory constraints, isolated converters such as DAB converters (Fig. 1a) appears as good technical solutions [1] especially with the bidirectional power transfers and the possible operating in ZVS/ZCS (Zero-Voltage Switching/Zero-Current Switching) depending on the operating point and the command used. However, the important operating switching frequencies of these converters impose a strict knowledge of the switching losses to avoid overheating. Consequently, it is vital to possess an accurate and quick tool to estimate the switching losses for any converter configuration and operating point.

The methods used today for semiconductor loss estimation are always a trade-off between accuracy of results versus computation time and the model building time. In this paper, a novel and generalist method based on mixed simulation [2] is presented to estimate the switching losses applied to DAB converters. It is based on perfect switches to simulate the waveforms and the allocate the switching energy loss stored in a lookup table. This approach is used in GT-PowerForge, an innovative software to design power converters [3].

The proposed methodology is an enhancement of the procedure presented in [2] and is illustrated in Fig. 1b. The main issue with this methodology is the inability to handle ZVS and hard-switching losses estimation within a given period. Indeed, in ZVS the switches are only controlled for turn-off while the turn-on is caused by the diode "natural" turn-on in parallel with the transistor. In hard switching, the switches are controlled for both turn-on and turn-off. However, in switching energy map based approach such as presented in [2] or used in PSIM or PLECS software, the turn-off energy is tabulated and used the same way for both hard and soft switching. Losses energies are typically provided in the semiconductor datasheet or obtained by double pulse test (measured or virtually obtained). This test is known to overestimate the turn-off value by measuring the stored energy into the output capacitance in addition to the dissipated energy [4]–[8]. Other measurements need to be implemented to obtain the soft-switching energies as presented in [5], [6]. Two different datasets of hard and soft switching energies are needed to estimate the losses as the two kinds of switching can coexist in a given operating sequence.

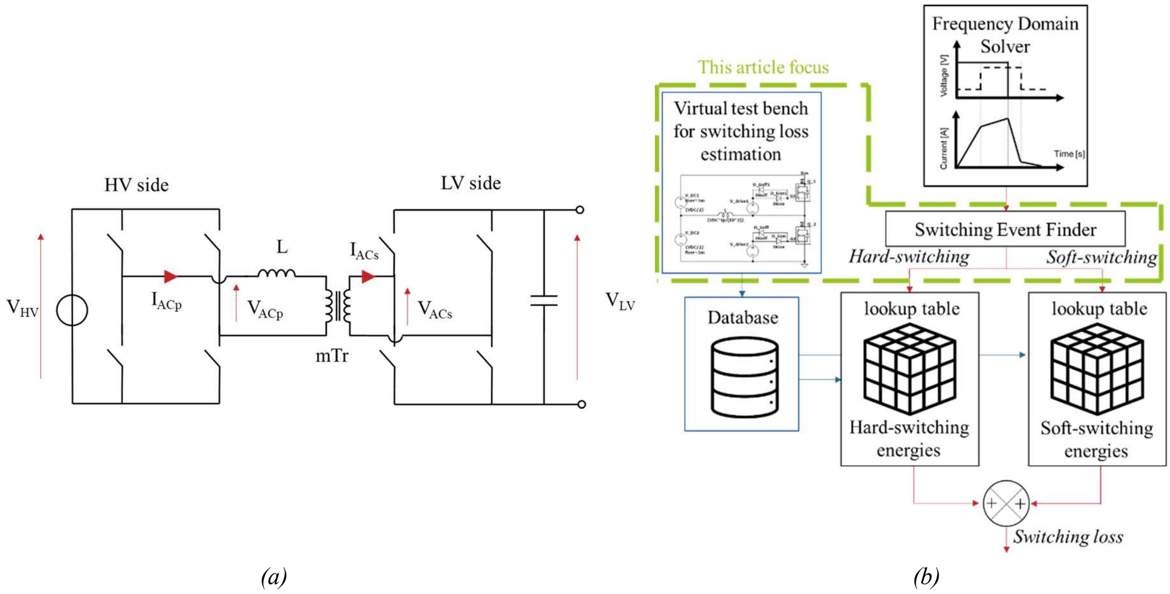

Figure 1: (a) Dual Active Bridge converter with H-bridge on both sides (b) switching losses estimation procedure to handle both hard and soft switching data.

In a first part, the motivation to propose this method is discussed. In a second part, loss estimation algorithm is presented. In a third part, the switching energies estimation is explained. In a fourth part, the results are compared to the literature and the limitations discussed.

Switching losses estimation procedure

The procedure to handle the two switching types (hard and soft switching) is as follow: at first, the waveforms are generated with a fast frequential MNA solver presented in [9] with perfect switch model. Then, the switching instants, the type of switching, and the switched voltage and current are estimated based on the waveforms. The switching losses at each switching instants are estimated based on this information by using lookup tables of the switching energies stored into a database, one for hard-switching and the other for soft-switching. The soft switching energies estimation will be discussed in the next section. Finally, all the losses are summed for each switching instant. This algorithm is also included into an electro-thermal convergence loop as discussed in [2].

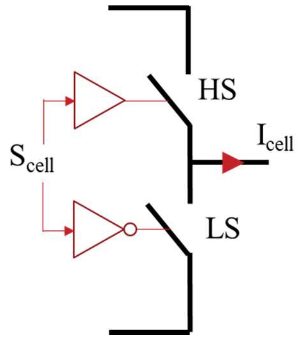

Figure 2: Switching cell conventions

Table I: Controlled switching events

	$S_{cell}\uparrow$	$S_{cell}\downarrow$
$I_{cell} > 0$	HS turn-on	HS turn-off
$I_{cell} < 0$	LS turn-off	LS turn-on

To find the type of switching (hard or soft) a switching event algorithm has been developed and is based on the switching cell concept introduced back in the 70s [10]. The Low Side switch (LS) and the High

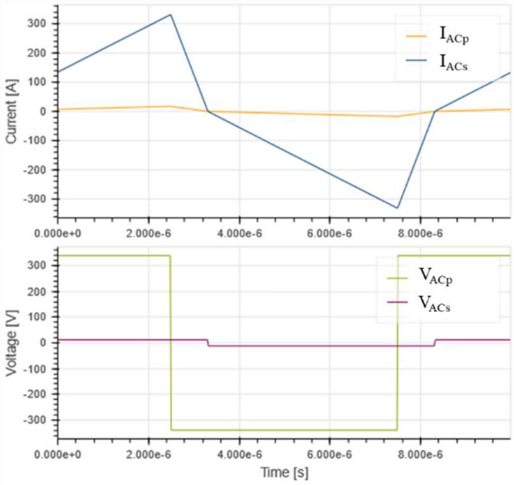

Figure 3: Simulated waveforms at V_{LV}=12V, V_{HV}=340V, P=2kW, L=26.7µH, mTr=19.

Side switch (HS) are commanded with the signal S_{cell} as presented in Fig. 2. If $I_{cell} > 0$ and S_{cell} present a rising edge ($S_{cell}\uparrow$), HS will have a controlled switch-on. This approach is generalized for all the cases in Table 1. The "natural" turn-on of a diode is not accounted as it is supposed lossless. The natural turn-off loss caused by diode recovery is accounted at the same time as the controlled turn-on loss. In a case of the usual rotation of controlled turn-on/turn-off, the hard-switching energies lookup table is used to estimate the loss. Indeed, as explained above, the classical double pulse test energies (Eon, Eoff) can only the used in pair because of the Coss stored energy. However, in a case of more than one consecutive controlled turn-off without controlled turn-on, the output capacitance energy is given back to the system, but it is still accounted as a loss in the double pulse measured turn-off energy (Eoff). In this case, the converter is in a ZVS condition, and the soft-switching data is chosen. The main advantage of this method lays in the flexibility in switching energy data handling and fast simulation capabilities. However, getting soft-switching data can be a bottleneck to this approach as it is not a data supplied by the manufacturer. Furthermore, the near zero current switching can imply incomplete soft-switching which is not handled at this level of the procedure but can be handled at the soft-switching energies data level. In the next section, the loss estimation algorithm will be validated by using measured soft-switching losses extracted form [11]. To address these issues, a simulation approach to estimate soft-switching energies for MOSFET will be presented in a further section.

The switching energies are stored in lookup tables, $E_{off|on|rr}(I, V, T_j)$ for hard-switching energies and $E_{soft}(I,V,T_j)$ for soft-switching energies. The data is interpolated or extrapolated linearly to estimate the energies at every switching instant.

The proposed procedure is compared to the literature [11] in two steps: first, the semiconductor loss estimated are compared with [11] using the switching energy curves presented in [11]. This comparison is done in the next section. In a second step, the losses are compared with energy curves estimated from simulation.

Semiconductor losses estimation for Dual Active Bridge compared to literature with the same loss curves

Table II: Switching losses comparison with same energies lookup tables

Results owners	LV Cond. loss	LV Sw. loss	LV total loss	HV Cond. loss	HV Sw. loss	HV Total loss	Total Loss HV+LV
Ref [11] (W)	25	6	31	15	9	24	55
With same energy data (W)	21.1	7.5	28.6	13.2	11.4	24.5	53.2
Difference (W)	3.9	-1.5	2.4	1.8	-2.4	-0.5	1.8
Difference (%)	15%	-25%	8%	12%	-26%	-2%	3%

A DAB with the topologies displayed in Fig.1a is compared with V_{LV}=12V, V_{HV}=340V, P=2kW, L=26.7µH, transformer ratio=19 with the semiconductor package imposed at 25ºC. The LV side includes 8 IRF2804 [12] in parallel and for the HV side the SPW47N60CFD [13]. The switching frequency is 100 kHz. The simulation is done with GT-PowerForge solver. The waveforms are displayed in Fig.3. The results are presented in Table II. The estimated total semiconductor loss is 3% lower than

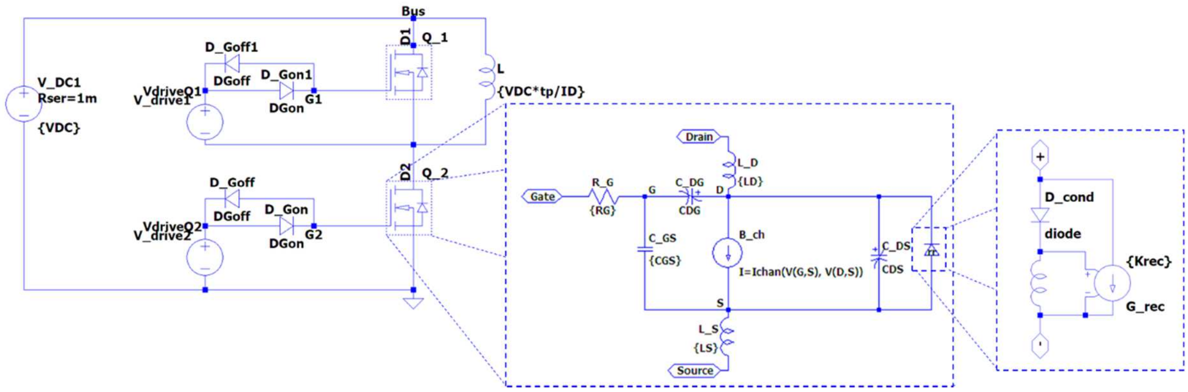

(a) *(b)* *(c)*

Figure 4: Proposed virtual double pulse test bench. (a) double pulse circuit. (b) MOSFET Model. (c) Body diode model.

the reference, the error being small, the proposed method is considered to be validated. In detail, the conduction losses and switching losses compensate themselves. The switching losses are overestimated which is coherent as the author in [7] proposed a method lowering the estimated switched current energies as the one used in the proposed simulation. The conduction losses are underestimated compared to the literature. The proposed results seem closer to reality as it is based on a more complex model as explained and compared in [2]. It can be noted that the converter losses are compared to the simulation done by the author in [11] and not to measurement. However, the author in [11] estimates the all-converter losses to be 6% higher than the measurement.

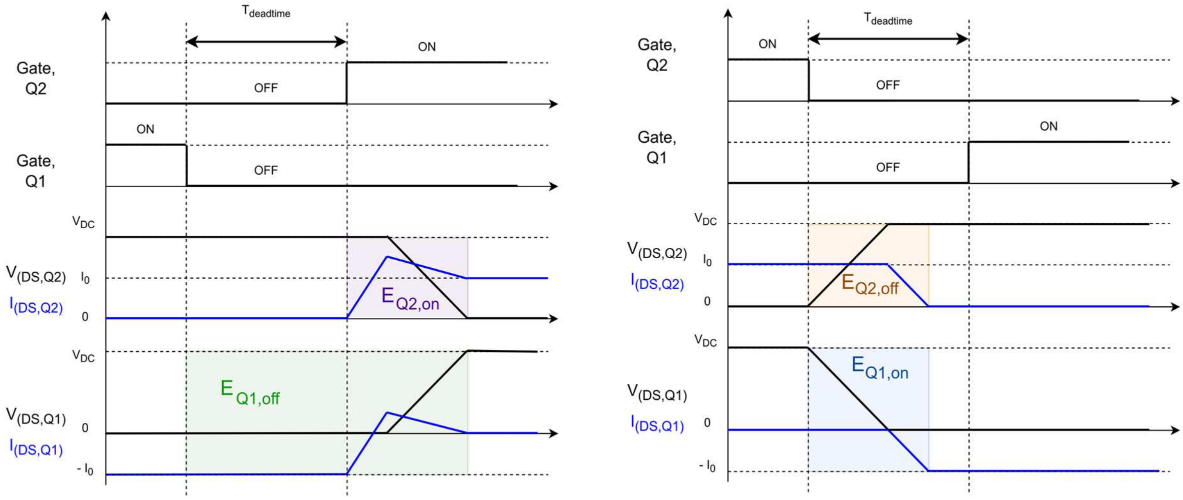

(a) *(b)*

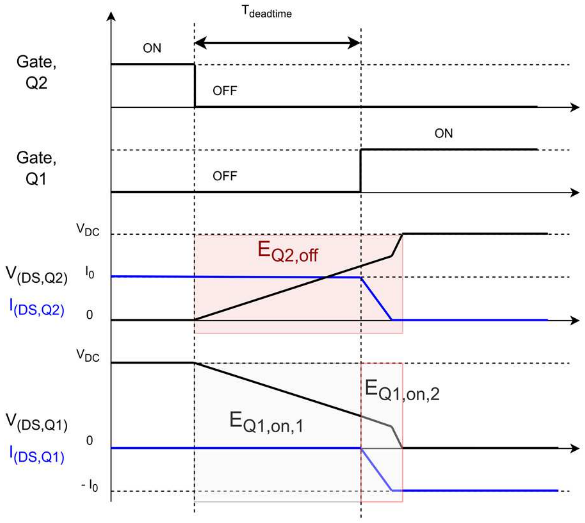

(c)

Figure 5: ideal switching waveforms to illustrate the measurement procedure (a) controlled turn-on of Q2 (b) controlled turn-off of Q2 which satisfied the ZVS condition (c) incomplete turn-off of Q2

Switching energies estimation based on double pulse simulation

The data can be extracted from manufacturer datasheets or from measurement results. However, when the data is not available, double pulse simulations are performed for MOSFET devices based on a LTSPICE MOSFET model as explained in [2] and displayed in Fig. 4b and Fig. 4c. The LTSPICE model parameters are fitted on the datasheet, especially for transconductance and diode parameters. The parasitic capacitances values are lookup table extracted from the same datasheet. The parasitic common source inductance which is known to be a key parameter for switching losses estimation [14], [15] is estimated based on the package used [16]–[18]. It can be noted that this virtual test bench can be used with LTSPICE model given by semiconductor device manufacturers, but convergence issues can happen.

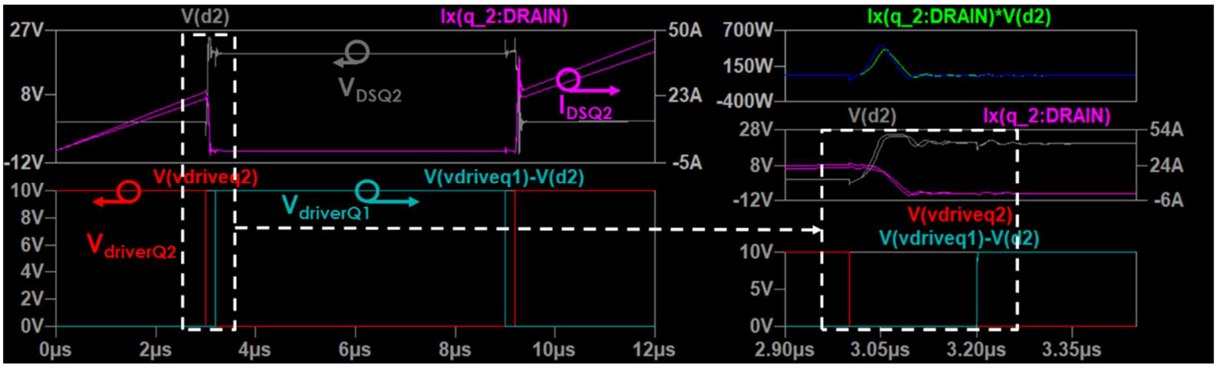

(a) *(b)*

Figure 6: (a) simulated waveforms for multiple target current, drain bias and temperature. (b) zoom in the switching instant with the deadtime illustration as well as the measured turn-off power.

For soft-switching energy measurement, a modified double pulse measurement is used as explained in [11], the circuit is displayed in Fig. 4a. At the start, Q2 is ON and Q1 OFF, the current will rise to the target switched current at the turn-off time for Q2. After a deadtime, the device Q1 is switching on. During device switch-off, the energy is measured for both Q1 and Q2 devices as presented in Fig.5b if the turn-of ends before Q1 is turned on after the deadtime (ZVS condition) as a result, Esoft is defined as Esoft = EQ2,off + EQ1,on. The simulated waveforms obtained with LTSPICE in Fig. 6 for 2 different current I_{DS}. However, if the ZVS condition is not fulfilled, an incomplete turn-off [6] append as presented in Fig. 5c and Esoft is defined as Esoft = EQ2,off + EQ1,on,1 + EQ1,on,2. The effect of deadtime on the blocking energy (Esoft) for a given switched current is shown in Fig.7a. With a sufficient deadtime, the energy is not impacted by it.

During the double pulse simulation, the turn-on and recovery losses energies are also estimated as

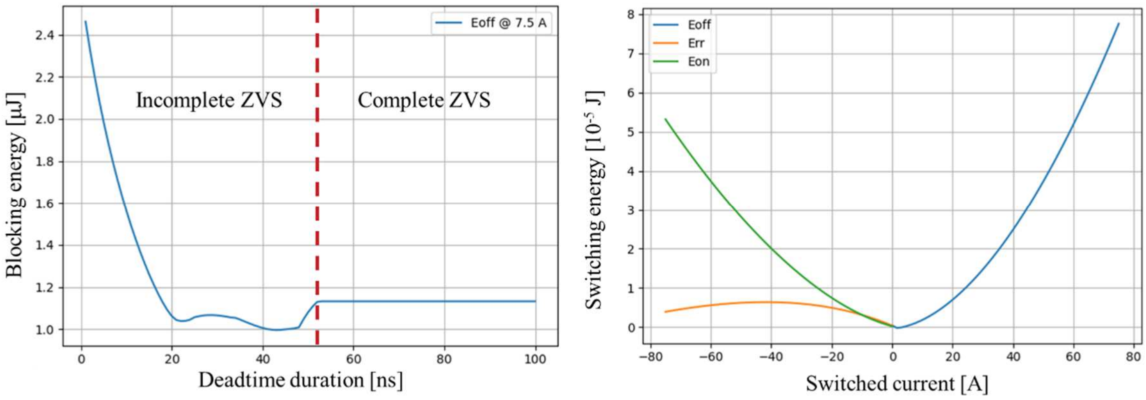

(a) *(b)*

Figure 7: (a) Effect of deadtime over the blocking energy for a given switched current (7.5A) (b) switching energies simulated for the device IRF2804 with a deadtime of 200 ns.

presented in Fig. 7b and are defined as Eon = EQ2,on and Err = EQ1,off, it can be noted that Err depends on the deadtime as conduction loss occurs during the deadtime.

Semiconductor losses estimation for Dual Active Bridge compared to literature with loss curves extracted from virtual double pulse test

Based on the procedure presented in Fig.1b, the waveform generated by GT-PowerForge frequential solver in Fig.3 and the switching energies data estimated based on the double pulse simulation presented in the previous section, the DAB loss are estimated and compared again against [11], the results are summarized in Table III. The total semiconductor losses are 16% lower with the results presented in this article. The conduction losses are identical as the results presented in Table II as the data used are the same. However, the error for switching losses are more pronounced (79% and 56%). Especially for LV switching loss the difference can be explained as the switching energies are measured for 8 devices directly in parallel in [11] while the simulation performed in the previous section is done with 1 device in parallel as this kind of simulation is very much dependent on the parasitic elements (especially the common source inductance) put 8 devices in parallel in a PCB will certainly impact a lot the results. A way to reduce this difference would be to recalibrate the LTPSICE model with the appropriate parasitic element or improve the used SPICE model. This model recalibration will be addressed in future work. However, proposed model has the great advantage to only rely on public available data to build the model, allowing a fair benchmark of the available semiconductor device in the market and identify the right trade-off for power converter design.

Table III: Switching losses comparison with energies lookup tables from LTSPICE virtual test bench

Results owners	**LV Cond. loss**	**LV Sw. loss**	**LV total loss**	**HV Con. loss**	**HV Sw. loss**	**HV Total loss**	**Total Loss HV+LV**
Ref [11]**(W)**	25	6	31	15	9	24	25
With energies from simulation (W)	21.0	1.3	22.3	13.1	14.0	27.1	21.0
Difference (W)	4.0	4.7	8.7	1.9	-5.0	-3.1	4.0
Difference (%)	16%	79%	28%	13%	-56%	-13%	16%

Conclusion

In conclusion, to obtain results more faithful to reality for converters operating in both hard and soft switching, a novel and integrated approach to estimate soft-switching losses is presented and compared to the literature for a DAB converter. The results are aligned with what is expected and the simulation is performed in less than 4s. The goal of obtaining a fast and more accurate method to estimate power converter switching losses in hard and soft switching is fulfilled. The proposed model and virtual double pulse setup allow the fair comparison of the semiconductor device removing the tedious and costly process of hardware measurement in a pre-design phase at the cost of a loss in precision in the results. This method is generic for all kinds of devices if the soft-switching data is available. However, only the MOSFET models is currently supported by the virtual test bench and it needs to be extended to other devices such as GaN devices and IGBTs as their behavior is strongly different from the MOSFET in soft-switching [19].

References

[1] F. Krismer, J. Biela, and J. W. Kolar, “A comparative evaluation of isolated bi-directional DC/DC converters with wide input and output voltage range,” in *Fourtieth IAS Annual Meeting. Conference Record of the 2005 Industry Applications Conference, 2005.*, Hong Kong, China, 2005, vol. 1, pp. 599–606. doi: 10.1109/IAS.2005.1518368.

[2] G. Fontes, F. Boige, A. Morentin, G. Delamare, T. Meynard, and N. Videau, “Semiconductor loss estimation in an innovative global power converter designer,” in *PCIM Europe digital days 2020; International Exhibition and Conference for Power Electronics, Intelligent Motion, Renewable Energy and Energy Management*, Jul. 2020, pp. 1–7.

[3] “PowerForge - Software for Power Converters,” *PowerForge*, Dec. 20, 2019. http://www.powerdesign.tech/ (accessed Dec. 20, 2019).

[4] S. Lefebvre, F. Costa, and F. Miserey, “Influence of the gate internal impedance on losses in a power MOS transistor switching at a high frequency in the ZVS mode,” *IEEE Trans. Power Electron.*, vol. 17, no. 1, Art. no. 1, Jan. 2002, doi: 10.1109/63.988667.
[5] D. Rothmund, D. Bortis, and J. W. Kolar, “Accurate Transient Calorimetric Measurement of Soft-Switching Losses of 10-kV SiC mosfets and Diodes,” *IEEE Trans. Power Electron.*, vol. 33, no. 6, Art. no. 6, Jun. 2018, doi: 10.1109/TPEL.2017.2729892.
[6] M. Kasper, R. Burkat, F. Deboy, and J. Kolar, “ZVS of Power MOSFETs Revisited,” *IEEE Trans. Power Electron.*, pp. 1–1, 2016, doi: 10.1109/TPEL.2016.2574998.
[7] F. Krismer and J. W. Kolar, “Accurate Power Loss Model Derivation of a High-Current Dual Active Bridge Converter for an Automotive Application,” *IEEE Trans. Ind. Electron.*, vol. 57, no. 3, Art. no. 3, Mar. 2010, doi: 10.1109/TIE.2009.2025284.
[8] J. C. Brandelero, “Conception et réalisation d’un convertisseur multicellulaire DC/DC isolé pour application aéronautique,” phd, 2015. Accessed: May 18, 2022. [Online]. Available: http://ethesis.inp-toulouse.fr/archive/00003097/
[9] G. Fontes *et al.*, “Fast Solver to Get Steady-State Waveforms for Power Converter Design,” in *PCIM Europe 2018; International Exhibition and Conference for Power Electronics, Intelligent Motion, Renewable Energy and Energy Management*, Jun. 2018, pp. 1–7.
[10] S. Cuk and R. Middlebrook, “A general unified approach to modelling switching DC-tO-DC converters in discontinuous conduction mode,” in *1977 IEEE Power Electronics Specialists Conference*, Palo Alto, CA, USA, Jun. 1977, pp. 36–57. doi: 10.1109/PESC.1977.7070802.
[11] F. Krismer, “Modeling and optimization of bidirectional dual active bridge DC-DC converter topologies,” Doctoral Thesis, ETH Zurich, 2010. doi: 10.3929/ethz-a-006395373.
[12] I. T. AG, “IRF2804 - Infineon Technologies.” https://www.infineon.com/cms/en/product/power/mosfet/n-channel/irf2804/ (accessed Dec. 06, 2021).
[13] I. T. AG, “SPW47N60CFD - Infineon Technologies.” https://www.infineon.com/cms/en/product/power/mosfet/n-channel/500v-950v/spw47n60cfd/ (accessed Dec. 06, 2021).
[14] D. Reusch, “Impact of Parasitics on Performance,” p. 5, 2020.
[15] Bo Yang and J. Zhang, “Effect and utilization of common source inductance in synchronous rectification,” in *Twentieth Annual IEEE Applied Power Electronics Conference and Exposition, 2005. APEC 2005.*, Austin, TX, USA, 2005, vol. 3, pp. 1407–1411. doi: 10.1109/APEC.2005.1453213.
[16] “Features and Benefits of 650 V CoolMOS™ C6 / E6.” Infineon application note.
[17] “650 V CoolMOS™ C7 Gold in TOLL package.” Infineon Product Brief.
[18] J. Zhang, “Choosing The Right Power MOSFET Package.” International Rectifier application note.
[19] G. Ortiz, H. Uemura, D. Bortis, J. W. Kolar, and O. Apeldoorn, “Modeling of Soft-Switching Losses of IGBTs in High-Power High-Efficiency Dual-Active-Bridge DC/DC Converters,” *IEEE Trans. Electron Devices*, vol. 60, no. 2, Art. no. 2, Feb. 2013, doi: 10.1109/TED.2012.2223215.